9th International Conference on Short and Medium Span Bridges
Calgary, Alberta, Canada, July 15-18, 2014

LARGE-SCALE FATIGUE TESTING OF CONCRETE HOLLOW BOX GIRDER DECK SLABS UNDER AXLE LOADS

Dipl.-Ing. Gregor Borkowski
Lucerne University of Applied Sciences and Arts – Competence Centre Structural Engineering
Horw, Switzerland

Prof. Dr. sc. techn. Karel Thoma
Lucerne University of Applied Sciences and Arts – Competence Centre Structural Engineering
Horw, Switzerland

B. Sc. Patrick Roos
Lucerne University of Applied Sciences and Arts – Competence Centre Structural Engineering
Horw, Switzerland

ABSTRACT

The conservation of existing structures including maintenance, assessment and, if necessary, strengthening is a current challenge for engineers. For the evaluation of the load carrying capacity and the remaining service life, detailed knowledge of the structural behaviour especially due to proceeding fatigue damage is required. In this paper, concrete deck slabs of hollow box girder bridges subjected to vehicle axle loads are examined.
The paper presents test results from a large-scale experiment on concrete deck slab specimens under cyclic loading. The test specimens have a span of 12m and a width of almost 6m. The axle loads (Swiss Code loads) are simulated using three hydraulic cylinders, which act one after another.
First, the experimental procedure is presented. Second, test results especially the calculation of the experimentally determined bending moments in the deck slab are shown. These results are calculated with an in-house software tool which is verified by recalculating the results of several slab tests.
Finally, it is discussed how the structural behaviour of deck slabs changes due to proceeding fatigue damage in the structure. This research project aims at contributing towards a better judgment of whether the service life of a bridge can be reached or strengthening is necessary.

1. INTRODUCTION

1.1 Initial Situation

The construction of prestressed concrete bridges started in the 1940s and reached its peak in the 1960s. By that time, the need for new bridges was increasing and the prestressing technology was extensively being taken advantage of. Today, increasing traffic loads and serious durability problems require regular inspections of the bridges. Since the planned service life of most of these bridges has not been reached, it is often more economical to maintain and strengthen, rather than replace them.
In 2009 a study on segmental bridges built between 1958 and 1976 was published (Buschmayer, W. et al. 2009). The study shows that almost 90% of the reviewed bridges exhibited cracks or damaged coupling joints and strengthening would be necessary. The question arises whether global or local strengthening of such bridges is really necessary or whether corrosion protection might be sufficient.
If strengthening is necessary, first it needs to be determined what stresses are acting on the bridge and what mode of failure governs: Failure by reaching the ultimate load or fatigue.

1.2 Research Objectives

In general, existing bridges are assessed using presently valid design loads. Due to constantly increasing traffic loads, the design loads in the present design standards are considerably higher than the design loads, which were used at the time of construction of the bridges. This means that often the requirements for the ultimate limit state and the service limit state cannot be met. Even when using detailed numerical calculations with sophisticated models, the resistances of the structures are frequently found to be much smaller than the design actions (Borkowski, G., Sigrist, V., 2012).
For the assessment of existing bridges, fatigue requirements often govern. In many cases these requirements cannot be met because the methods in the design standards are based on strongly conservative assumptions. The research project presented in this paper seeks to address these issues.
Large-scale bending tests on slabs are used to analyse their load-bearing behaviour. In these tests, segments of bridge slabs are cyclically loaded until their bending reinforcement fails due to fatigue.
Three hydraulic jacks are used to simulate recurring vehicle crossings. The applied vehicle loads meet the size and geometrical specifications given in the relevant Swiss standard (SIA 261, 2003).
The aim of the research project is to provide monitoring methods for determining and assessing the damage process caused by fatigue. Further, it is planned to incorporate the gained knowledge in the relevant design standards.

2. EXPERIMENTAL INVESTIGATIONS

2.1 Specimen

The investigations focus on determining the load transfer within deck slabs. The test setup is based on the cross-sectional geometry and reinforcement detailing of older bridges (Tab. 1). The specimen dimensions can be seen in Figure 1.
The specimen represents the top slab of a box girder. As the bottom slab is missing in the test setup, the transverse stiffness of a box girder is reproduced with six prestressed (50 kN each) threaded rods (Figure 1 & 3). The test specimen is mounted on four 0.5 MN hydraulic jacks, so that its position can be adjusted during the test if necessary.

Table 1. Reinforcement in the specimen slab

Layer	Reinforcement: ------	
	Ø [mm]	spacing [cm]
Top transverse	14	20
Bottom transverse	10	20
Top longitudinal	10	20
Bottom longitudinal	14	20

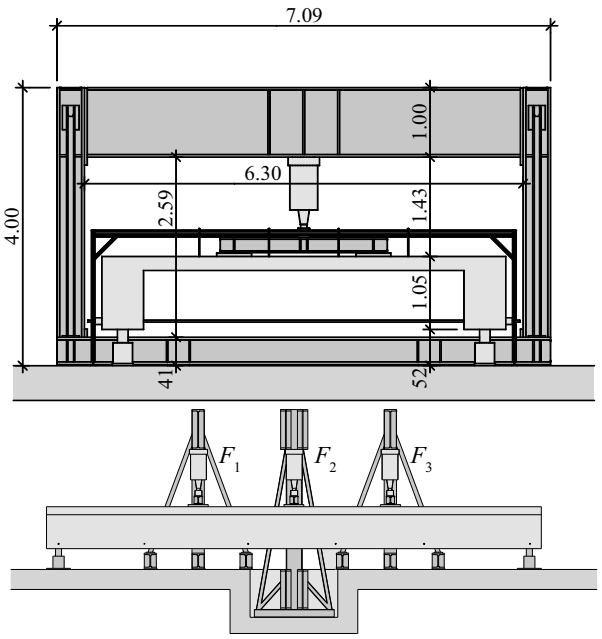

Figure 1. Top: Cross section; bottom: longitudinal section of the experiment set-up

2.2 Experimental Set-Up

The load is applied with three hydraulic jacks, which successively load the specimen. Therefore, during one load cycle the three jacks are applied one after another. Following the provisions given in the relevant Swiss standard (SIA 261, 2003), a transverse beam distributes each jack load to two load distribution plates. The transverse spacing between the plates is 2 m (Figure 1) and corresponds to the distance between the two point loads of an axle load as stipulated by the code.
The 270 kN load applied by each jack corresponds to the characteristic value of this axle load. In the longitudinal direction the distance between the jacks is 2.4m (Figure 1). The load history of one cycle is shown in Figure 2. As can be seen, the loads are applied successively, but a minimal load of 30 kN is always maintained at each jack so as to ensure that the testing equipment is never completely unloaded during the test.

Besides the continuous load and deformation measurements at the locations of the jacks, the vertical deformations of the test specimen at 16 locations and the force in the prestressed transverse rods are measured every five hours for 20 seconds. This means that the specimen deformations due to at least five full load cycles (fictitious vehicle crossings) can be measured (Figure 2). Details about the experimental setup can be found in Borkowski et. al (2013).

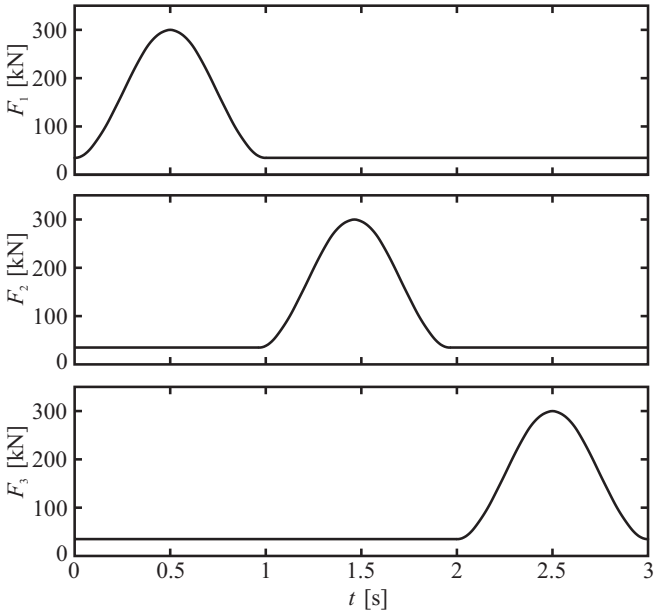

Figure 2. Load history for one cycle

3. TEST EVALUATIONS

3.1 Measurements

After every 500 thousand (500k) cycles the loading process is interrupted. During these breaks the surface deformations on the upper and lower slab face are measured with a hand-held mechanical strain gauge (measurement precision 4/1000 mm). The measurements are carried out three times on one half of the slab. Thereto each jack is loaded separately up to 300 kN and put into deformation control mode, while the other two jacks are maintained at 30 kN. The crack pattern is recorded at each load application so that the cracking progress is also documented after every 500k cycles.


Figure 3. Photo of the experiment setup

Figure 4 shows the recorded vertical slab deformations below each of the three jacks. The envelopes of the maximal and minimal deformation values are shown. The figure shows to which extent the test specimen exhibits residual deformations due to cyclic loading. It can also be seen that the specimen stiffness relative to the load is almost constant.

With a program especially designed for this purpose, which is based on the layer model for slabs according to (Kollegger, J., 1991, CEB, 2008, Seelhofer, H. 2009, Urweider, T., 2012), the cross-sectional strains, curvatures, steel stresses and bending moments in the slab can be determined from the deformation measurements taken with the hand-held mechanical strain gauge.

The strain measurements are carried out on both the top and the bottom surface of the slab. For this purpose, a square grid of measuring points orthogonally spaced at 200 mm is marked on the surface of the untested specimen. The locations of the measuring points are identical on both the top and the bottom surface (Figure 5). Orthogonal and diagonal measurements are carried out.

More measuring tracks are available than are needed to determine the positions of the individual measuring points with respect to each other. However, due to the measurement precision of 4/1000 mm, it is both possible and necessary to carry out linear error compensation using the theory of elastic systems (Linkwitz, K., 1961). The error compensation is carried out using the least-squares method by means of FEM. Hence, it is possible to use the measured values to determine the concrete strains at the plate surfaces.

3.2 Evaluation of the measurements

By subdividing the concrete slab into *n* layers as proposed by Kollegger, J., 1991, CEB, 2008 and Seelhofer, H., 2009 the measured concrete strains can be used to determine the cross-sectional curvature, reinforcement strains as well as the bending moments and hence the shear forces in the slab (Figure 6, Eq. [1]).

$$\varepsilon_x(z) = \varepsilon_{x0} + z \cdot \chi_x$$
$$\varepsilon_y(z) = \varepsilon_{y0} + z \cdot \chi_y \quad [1]$$
$$\gamma_{xy}(z) = \gamma_{xy0} + z \cdot 2\chi_{xy} = \gamma_{yx}(z)$$

Each layer is assumed to be a thin plate with a plane state of stress and small deflections compared to its thickness. The model also assumes that the reinforcement prevents brittle failure of the cross-section when the concrete cracks. Further, the cross-sections are assumed to remain plane and perpendicular to the *xy*-plane (Kirchhoff-Love-Theory) so that the strain state in each layer can be determined according to the relations in Figure 6 (Marti, P. et. al, 1998) [1]. Parameters ε_{x0}, ε_{y0} and γ_{xy0} in Figure 6 are the strains at the middle plane, and χ_x, χ_y and χ_{xy} are the bending and twisting curvatures of a plane plate element, respectively.

The effective area of the cracked concrete contributing to tension stiffening is assumed to extend from the cracked plate surface to a depth of twice the distance between the plate surface and the centre of gravity of the tension reinforcement. Tension stiffening is only considered in layers within this zone (Marti, P., 1990). Hence, the plate bending and twisting moments m_x, m_y and m_{xy} and the membrane forces n_x, n_y and n_{xy} can be calculated by integrating the stresses σ_x, σ_y, and τ_{xy} over the plate thickness (Figure 6 (b)).

Using the tension chord model (Alvarez, M., 1998), the cracked membrane model (Kaufmann, W., 1998) and the biaxial law for concrete (Stempniewski, L., Eibl, J., 1996), the stress state of an element can be determined. Combined with the layer model, the three models can be applied to reinforced concrete plates (Thoma, K. et al. 2014).

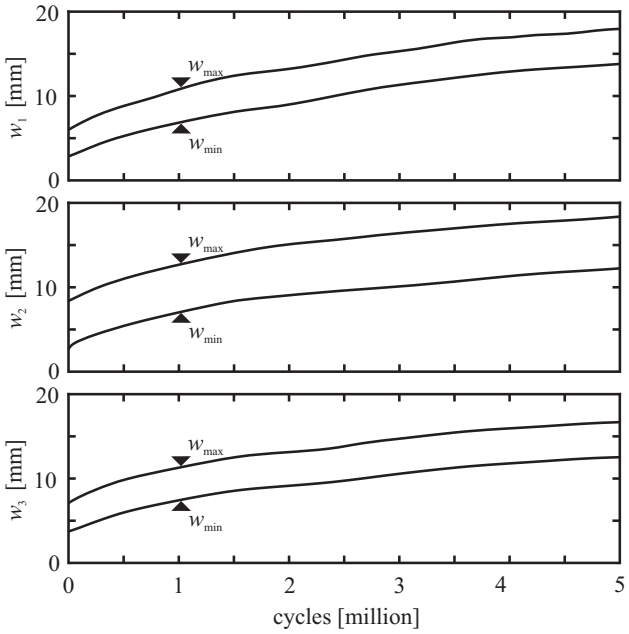

Figure 4. Vertical slab displacement vs. load cycles up to 5 million cycles

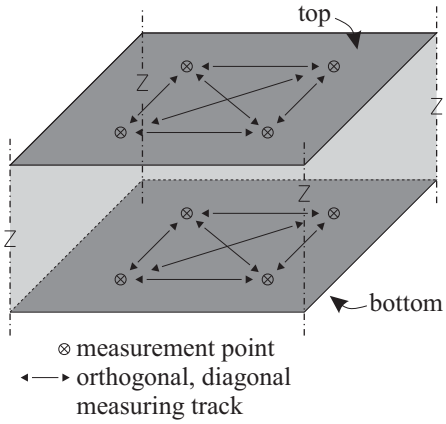

Figure 5. Slab section with measuring tracks

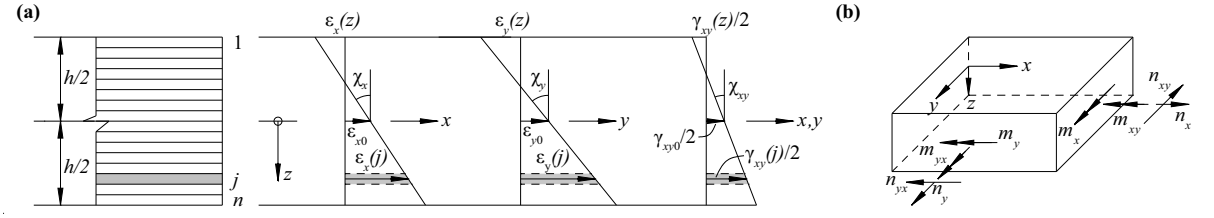

Figure 6. Layer model: a) Strains and curvatures of the plate element; b) Moments and forces in the plate element (Thoma, K. et al. 2014)

3.3 Verification of the analytical approaches

Experiments on concrete plates with mesh reinforcement were carried out at the Lucerne University of Applied Sciences and Arts. The objective of the tests was to determine the deformation capacity of mesh reinforced concrete plates. Three plates were tested. One plate was reinforced with steel bars and used as a reference; the two remaining plates contained steel mesh reinforcement. The analytical approaches described in the previous section are verified by recalculating the experimental results of the reference plate. The employed material properties are shown in Table 2.

The test specimen is 8.8 m long, 4.4 m wide and 0.2 m high. The load is applied with 24 hydraulic presses. The plate is supported on 41 load cells that are positioned uniformly around its edges and at the transverse centreline to act as intermediate supports (Fig. 7). With this support configuration, the plate only resists forces in the direction of the applied load. The edges are not prevented from lifting off the supports.

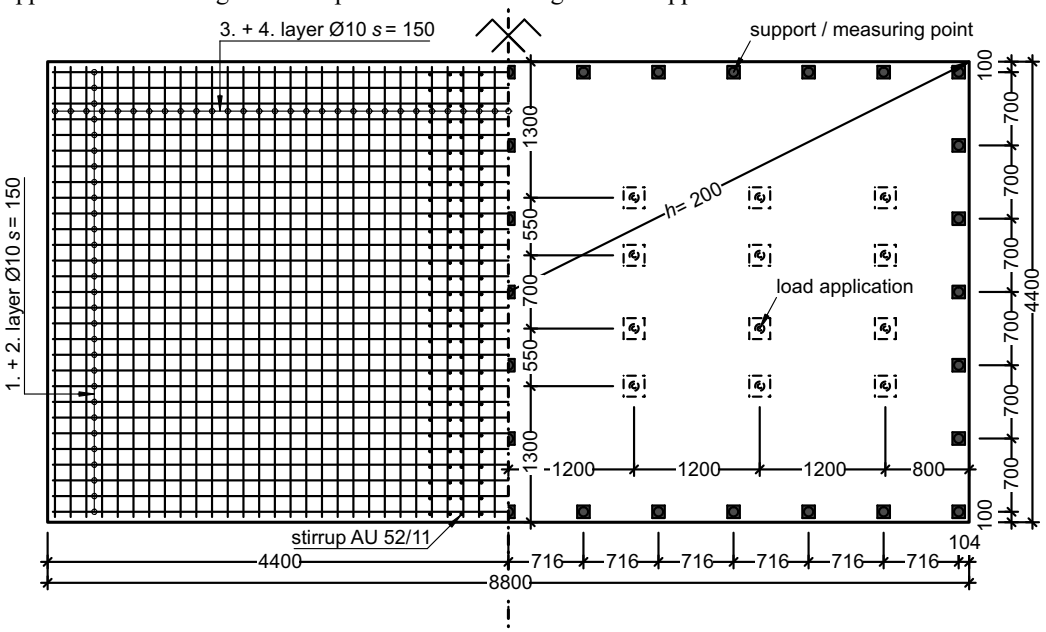

Figure 7. Test plate: geometry and reinforcement detailing (distances in mm)

The recalculation is carried out with the approaches described by Thoma, K. et al. (2014) using minimum and maximum crack spacings ($\lambda = 0.5$ and $\lambda = 1.0$, respectively).

A comparison of the load-deformation curves obtained experimentally and analytically is shown in Fig. 8. Good agreement is achieved between the calculated and the experimentally determined load-deformation curves in the cracked state. The FE model slightly overestimates the vertical displacements of the plate after yielding of the reinforcement.

In the following paragraph, the recalculated principal strains (using $\lambda = 0.5$) at the plate surfaces and the measured principal strains due to a load F = 717.3 kN are compared. The maximum and minimum measured principal strains at the top surface of the test plate are $\varepsilon_{1sup} = 14.02‰$ (at the intermediate supports) and $\varepsilon_{3sup} = -1.71‰$ (at midpanel), respectively. The corresponding recalculated values are $\varepsilon_{1sup} = 10.12‰$ and $\varepsilon_{3sup} = -1.30‰$. The measured values at the bottom surface of the test plate are $\varepsilon_{1inf} = 9.35‰$ at midpanel and $\varepsilon_{3inf} = -2.96‰$ at the intermediate

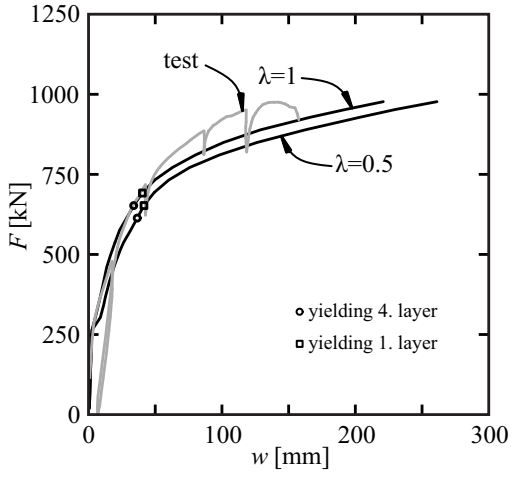

Figure 8. Load-deformation curves at midpanel

supports. The corresponding recalculated strains are $\varepsilon_{1inf} = 10.02‰$ and $\varepsilon_{3inf} = -1.91‰$ at midpanel and at the intermediate supports, respectively. Figure 9 shows the comparison of the principal strains. It can be seen that good agreement between the calculated and measured strains is achieved.

Table 2. Material properties for the test plate

Steel reinforcement:				Concrete:	
f_{sy} [MPa]	f_{su} [MPa]	ε_{su} [‰]	E_s [GPa]	f_{cc} [MPa]	ε_{cu} [‰]
445.6	558.6	80.8	196	28.61	3.0

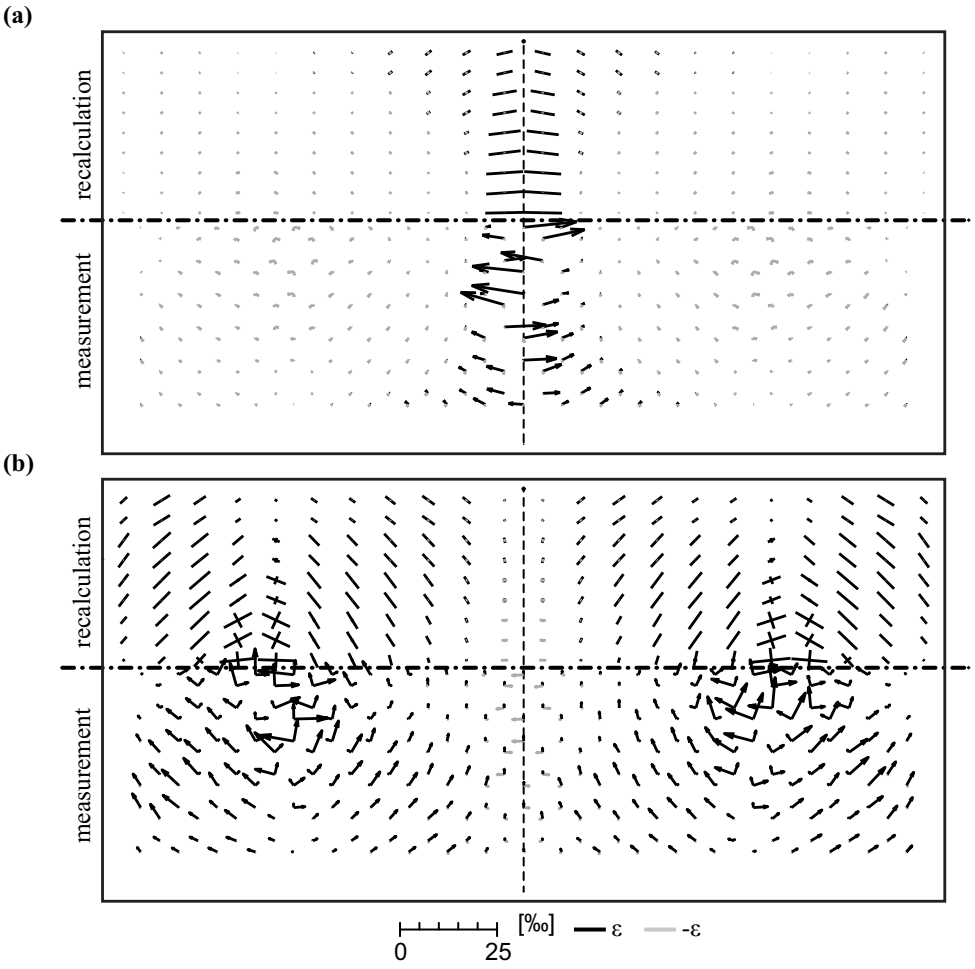

Figure 9. Comparison of the principal strains for load F_{tot} = 1‘434.6 kN: (a) Principal strains at the top surface of the plate; (b) Principal strains at the bottom surface of the plate

Fig. 10 (a) and Fig. 10 (b) show the principal strains, the crack pattern as well as the steel and concrete stresses in the cross-section of a midpanel element at the maximum load. The steel stresses in the two bottom layers of reinforcement at midpanel are $\sigma_{sxrinf} = 536.9$ N/mm^2 and $\sigma_{syrinf} = 510.3$ N/mm^2, respectively. Both values exceed the steel yield stress of $f_{sy} = 445.6$ N/mm^2. The concrete stresses at the top of the element is $-\sigma_{cxr} = -\sigma_{cyr} = 21.91$ N/mm^2, which is slightly higher than the compressive strength of the concrete $-f_c = 21.81$ N/mm^2.
In the FE model with an assumed maximum concrete strain of $\varepsilon_{cu} = -3.0‰$ the ultimate load is reached after concrete crushing at the intermediate supports. At the intermediate supports, the stress in the top layer of the reinforcement in the concrete cracks reaches 97.3% of the steel tensile strength. The ultimate load of the specimen obtained from the FE model is slightly smaller than the experimentally determined ultimate load.
Using the approaches by Thoma, K. et al. (2014) in a FE program, the load-deformation behaviour of reinforced concrete panels and plates can be described thoroughly. This is confirmed by recalculations of the results of various

experiments. Further, the stress states of reinforced concrete plate sections can be determined from the experimentally determined strain states.

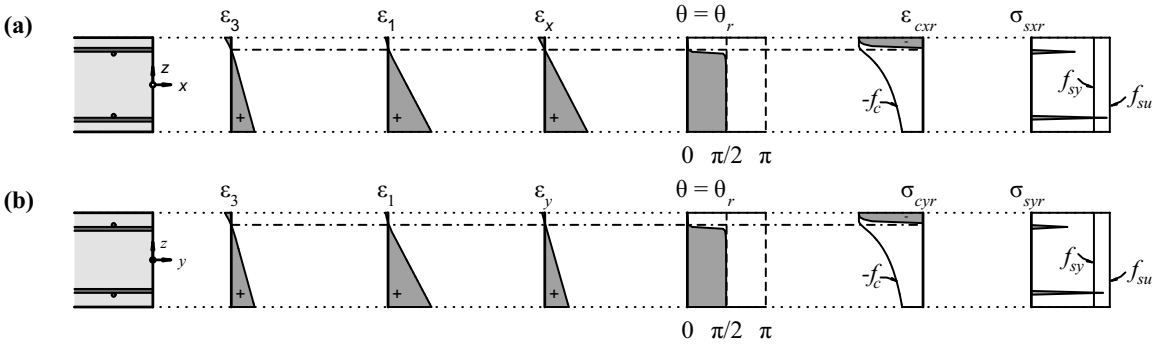

Figure 10. Cross-sectional analysis for a midpanel element at maximum load: (a) x-direction; (b) y-direction

3.4 Results of the fatigue test

The analytical approaches for reinforced concrete plates described in the previous section have been verified by recalculation of experimental results. Therefore, the internal forces in the tested plate can be calculated for each load level, and the influence of fatigue damage can be determined. The following images display the calculated bending moments of the plate due to a load applied by press F_1 (Fig. 1) after 500k load cycles (Fig. 13) and after 5 million load cycles (Fig. 14).

Comparing Fig. 13 and Fig. 14, it can be seen that the progressive cracking of the concrete causes the moments to shift towards the uncracked and hence stiffer areas at the centre of the plate (Fig. 12). As a result, the effective width of the plate decreases and the moments

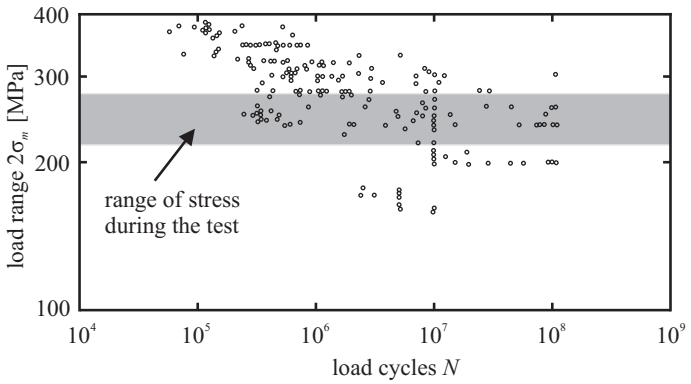

Figure 11. Wöhler diagram for steel bars with diameter d = 16 mm (Martin, H., Russwurm, D. 2001)

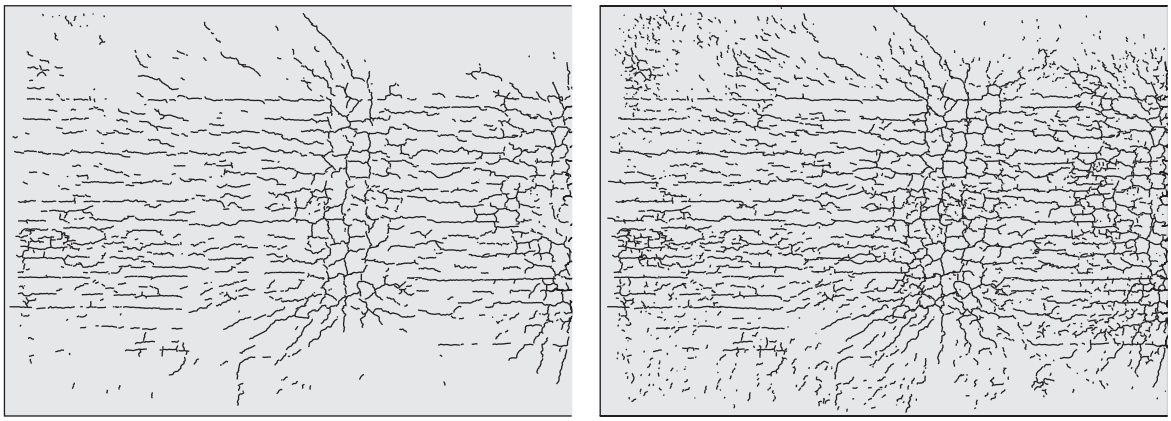

Figure 12. Crack patterns at the bottom surface of the plate (one half of the plate is shown), left side: after 500k load cycles; right side: after 5 million load cycles

increase. This causes the stresses in the reinforcement to increase, exacerbating the fatigue damage. An example of this stress increase can be seen in the bottom transverse reinforcement of the plate (Fig. 16). Further details can be found in Borkowski, G. et al. (2013).

Using the calculated steel stresses and Eq. [2], both the duration of the fatigue test as well as the fatigue life of reinforced concrete structures can be estimated (Fig. 11).

[2] $2\sigma_m = \sigma_{\max} - \sigma_{\min}$

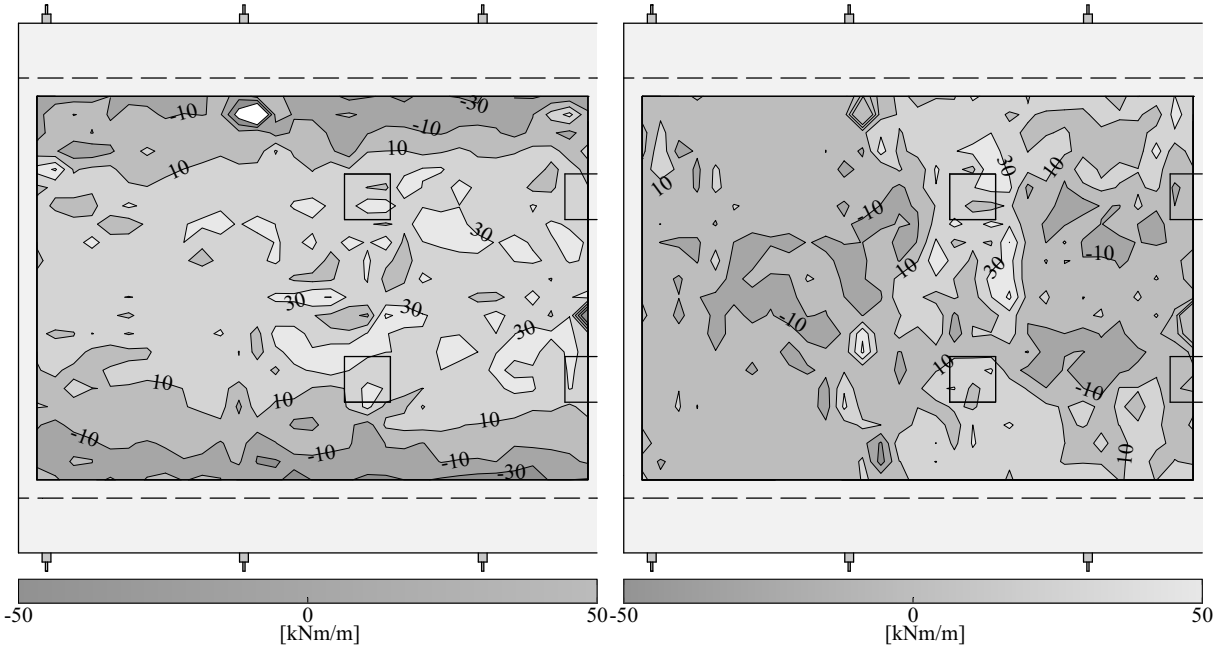

Figure 13. Bending moments after 500k load cycles (load F_1): left side: about the longitudinal axis; right side: about the transverse axis

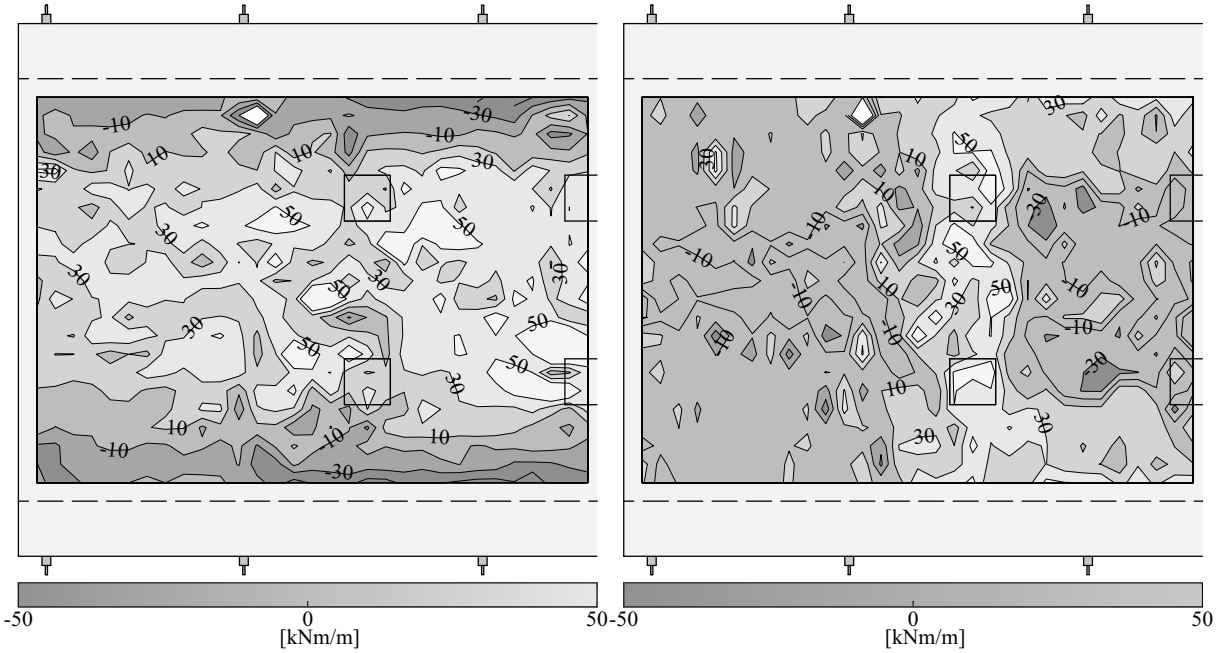

Figure 14. Bending moments after 5 million load cycles (load F_1): left side: about the longitudinal axis; right side: about the transverse axis

4. CONCLUSIONS AND FURTHER RESEARCH

The present research work comprises the execution and evaluation of large-scale tests on bridge deck slab members, which are subjected to fatigue relevant stress levels caused by vehicle axle loads. First, the general testing program is presented. The test specimen is described and the loading sequence is explained. Further, the components of the measuring program are presented and it is shown which data can be gained from the measurements. Finally, the stress levels in the slab bending reinforcement are illustrated.

By means of the experiment and the evaluation program it is possible to illustrate the load bearing behaviour in the slab due to possible fatigue damage of the reinforcement. It is planned to carry out at least three further tests on identical test specimens. These test specimens will be preloaded with tensile and compressive forces in the longitudinal and transverse directions, in order to be able to represent effects such as longitudinal and transverse bending in the span and support regions of the bridge.

The knowledge gained from this research project is intended to be incorporated in the Swiss Standard for the assessment of existing structures. On this basis, the load bearing capacity reserves of existing bridges can be more accurately determined and evaluated, in order to prevent unnecessary strengthening measures.

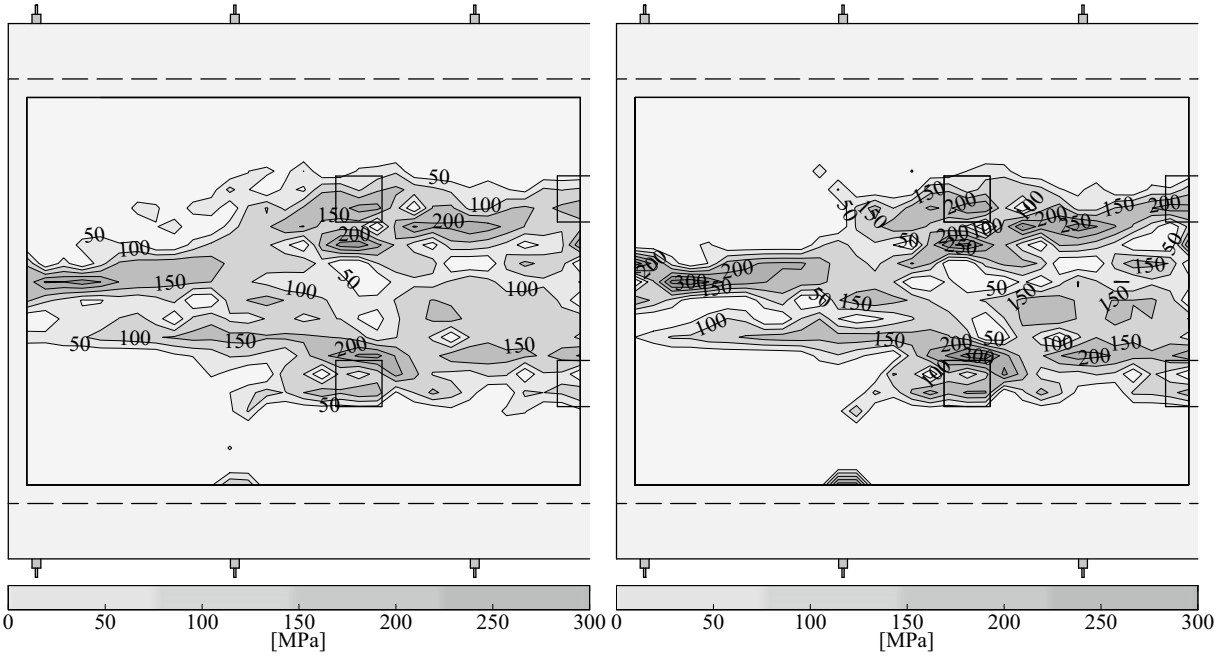

Figure 15. Stresses in the bottom reinforcement in transverse direction. Left side: after 500k cycles; right side: after 5 million cycles

5. ACKNOWLEGEMENTS

The authors thank the Swiss Federal Roads Office (ASTRA) for financing the project. This project is also being assisted by the University of Applied Science in Rapperswil under the supervision of Prof. Dr. techn. sc. A. Kenel.

6. REFERENCES

Alvarez, M. 1998. *Einfluss des Verbundverhaltens auf das Verformungsvermögen von Stahlbeton.* Institute of Structural Engineering. ETH Zurich. IBK Report No. 236. Birkhäuser Verlag. Basel, 182 pp.

Borkowski, G. Sigrist, V. 2012. Computational Assessment of Prestressed Concrete Bridges. *18th IABSE Conference Seoul.* South Korea, 8 pp. paper in CD-ROM proceedings.

Borkowski, G., Thoma, K., Roos, P. 2013. Full-Scale Testing of Concrete Deck Slabs under Fatigue-Causing Axle Loads, *SEMC 2013: The Fifth International Conference on Structural Engineering, Mechanics and Computation.* Cape Town, South Africa. 8 pp. paper in CD-ROM proceedings.

Buschmayer, W., Roder, C., Gusia. 2009. Erfahrungen bei der Beurteilung der Dauerhaftigkeit vorgespannter Bewehrung von älteren Spannbetonbrücken. *Bautechnik*, Vol. 86.

CEB Comité Euro-International du Béton. 2008. *Practitioners´ Guide to Finite Element Modeling of Reinforced Concrete Structures*. Bulletin State of the Art Report No. 45.

Kaufmann, W. 1998. *Strength and Deformations of Structural Concrete Subjected to In-Plane Shear and Normal Forces*. Institute of Structural Engineering, ETH Zurich. IBK Report No. 234. Birkenhäuser Verlag. Basel. 147 pp.

Kaufmann, W., Marti, P. 1998. Structural Concrete: Cracked Membrane Model. *ASCE Journal of Structural Engineering*. Vol. 124, No. 12., pp. 1467-1475

Kollegger, J. 1991. Algorithmus zur Bemessung von Flächentragwerkelementen unter Normalkraft- und Momentenbeanspruchung. *Beton- und Stahlbetonbau*, Vol. 86 p. 114.

Linkwitz, K. 1961. *Fehlertheorie und Ausgleich von Streckennetzen nach der Theorie elastischer Systeme.* Dissertation, Technische Hochschule München. Heft No. 46. Verlag der Bayerischen Akademie der Wissenschaften, Munich, 69 pp.

Marti, P. 1990. Design of Concrete Slabs for Transverse Shear. *ACI Structural Journal*, Vol. 87, No. 2, pp. 180-190

Marti, P., Alvarez, M., Kaufman, W., Sigrist, V. 1998. Tension Chord Model for Structural Concrete. *ASCE Journal of Structural Engineering.* Vol. 8, No. 4, pp. 287-298

Martin, H., Russwurm, D. 2001. *Betonstähle für den Stahlbetonbau*. Bauverlag BV.

Seelhofer, H. 2009. *Ebener Spannungszustand im Betonbau: Grundlagen und Anwendungen*. Institute of Structural Engineering, ETH Zurich. IBK Report No. 320. vdf Hochschulverlag.

Stempniewski, L., Eibl, J. 1996. *Finite Elemente im Stahlbeton.* Sonderdruck aus dem Betonkalender 1996. Ernst & Sohn Verlag. Berlin, pp. 577-647

Swiss Code SIA 261, 2003. Actions on Structures. *Swiss Society of engineers and architects.*

Thoma, K., Roos, P., Weber, M. 2014. Finite-Element-Analyse von Stahlbetonbauteilen im ebenen Spannungszustand, Scheiben- und Plattenberechnungen auf Basis des gerissenen Scheibenmodells. *Beton- und Stahlbetonbau*. In print.

Urweider, T. 2012. Plattenschnittkräfte auf Basis von Setzdeformetermessungen. *Master-Thesis, Lucerne University of Applied Sciences and Arts*